2023-01

An organotypic oral mucosal infection model to study host-pathogen interactions

Gould, SJ

10.1177/20417314231197310
Journal of Tissue Engineering
SAGE Publications

Original Article

An organotypic oral mucosal infection model to study host-pathogen interactions

Journal of Tissue Engineering
Volume 14: 1–14

DOI: 10.1177/20417314231197310
journals.sagepub.com/home/tej
Sage

Samantha J Gould[1], Andrew D Foey[2] and Vehid M Salih[3]

Abstract

Early *in vitro* oral mucosal infection models (OMMs) failed to consider the suitability of the model environment to represent the host immune response. Denture stomatitis (DS) is mediated by *Candida albicans*, but the role of *Staphylococcus aureus* remains uncertain. A collagen hydrogel-based OMM containing HaCaT and HGF cell types was developed, characterised and employed to study of tissue invasion and pro-inflammatory cytokine production in response to pathogens. Models formed a robust epithelium. Despite their inflammatory baseline, 24-h infection with *C. albicans*, and/or *S. aureus* led to tissue invasion, and significantly upregulated IL-6 and IL-8 production by OMMs when compared to the unstimulated control. No significant difference in IL-6 or IL-8 production by OMMs was observed between single and dual infections. These attributes indicate that this newly developed OMM is suitable for the study of DS and could be implemented for the wider study of oral infection.

Keywords

Candida albicans, *Staphylococcus aureus*, organotypic, oral mucosa, infection model, tissue-engineering, denture stomatitis

Date received: 1 May 2023; accepted: 10 August 2023

Introduction

The oral immune system is compromised by denture wear. Reduced salivary flow between the denture and the hard palate inhibits the sloughing of epithelial cells and delivery of salivary antimicrobial factors.[1–4] Denture wear can lead to tissue trauma, especially if improperly fitted, compromising the integrity of the epithelial barrier. Additionally, acrylic dentures may support biofilm formation, particularly when inadequately or infrequently cleaned.[5]

The fungus *Candida albicans* is a frequent oral coloniser and a common cause of infection.[4] *C.albicans* is the main causative agent of Denture Stomatitis (DS), which presents as erythema and oedema in oral tissues that underlie dentures, most notably the hard palate.[3] Locally, the recognition of pathogens, mostly due to damage, by epithelial cells and myeloid cells including tissue resident macrophages and dendritic cells, leads to localised inflammation of the hard palate, which in more severe cases can lead to more generalised inflammation of the oral cavity.[6] DS associated biofilms are thought to be potential reservoirs for disseminated infection, therefore all DS cases should be considered of clinical importance.[7–9]

Concurrent bacterial infections are common and may contribute to disease severity. *Staphylococcus aureus* is a commensal bacterium that can act as an opportunistic pathogen. *S.aureus* is now an accepted member of the normal oral flora and has been detected in conjunction with *C.albicans* in the oral cavity, and is thought to be associated with DS .[10–12] More recently, small colony variants of *S.aureus* were found to associate with *C.albicans* amongst

[1]Department of Clinical and Biomedical Sciences, University of Exeter, Exeter, Devon, UK
[2]School of Biomedical Health Sciences, University of Plymouth, Plymouth, Devon, UK
[3]Peninsula Dental School, University of Plymouth, Plymouth, Devon, UK

Corresponding author:
Vehid M Salih, Peninsula Dental School, University of Plymouth, Drake Circus, Plymouth, Devon PL4 8AA, UK.
Email: vehid.salih@plymouth.ac.uk

denture wearers.[13] Elsewhere, *S.aureus* infections range from superficial, localised wound infections to systemic sepsis, all of which are dependent on a portal of entry through the epithelial barrier.[14] *C.albicans* and *S.aureus* are considered to have a synergistic relationship in terms of virulence and disease severity.[15–17] It has also been proposed that *S.aureus* may be able to hitch a lift across the mucosal barrier by adhering to *C.albicans*, risking *S.aureus* gaining access to deeper tissues and subsequently the blood stream.[18–22]

C. albicans contains multiple cell wall components that possess conserved structural motifs including chitin, glucans and mannans, which are exposed to the extracellular environment, as well as internal nucleic acid sequences, all of which may act as PAMPs and are subsequently detected by pattern recognition receptors (PRRs) .[23–31] Gram positive bacteria such as *S.aureus* possess multiple cell-wall components that act as PAMPs including *lipoteichoic* acid and peptidoglycan, which are recognised by TLR-2.[32,33] TLR-2 is expressed at the cell surface of oral keratinocytes, gingival fibroblasts and *in vivo* on innate immune cells, and can recognise both *C.albicans* and *S.aureus*, in conjunction with other PRRs.[25,32–35] Upon pathogenic recognition, epithelial cells and immune cells secrete cytokines, which instigate an immune response, including further immune cell recruitment and, in the case of a functional immune system, ultimately pathogenic clearance and tissue repair.

At the oral mucosal barrier, keratinocytes and local resident immune cells such as macrophages and Langerhans cells possess pattern recognition receptors such as Toll-Like-Receptors (TLRs), which recognise conserved pathogen associated molecular patterns (PAMPs), and damage associated molecular patterns (DAMPs).[36,37] Upon TLR activation, cytokines are produced. Depending on the local cytokine *milieu*, an immune response is orchestrated. This may lead to the recruitment of further innate immune cells for pathogenic clearance, differentiating naïve immune cells into their specific and activated counterparts and presenting pathogenic antigens to the adaptive immune system to instigate a memory response.

Pro-inflammatory cytokines play a key role in instigating an immune response at the oral mucosal barrier. Interleukin 6 (IL-6) is a multifunctional cytokine that is paramount to a functional immune response. It undertakes both inflammatory and regulatory roles and is required to maintain tissue health. IL-6 is secreted by many cell types, including immune cells, oral epithelial cells and fibroblasts, and the IL-6 receptor (IL-6R) is expressed on a multitude of cell types.[38] IL-6 is also important for regulating wound healing; and dysregulation of IL-6 can lead to either fibrotic or chronic wounds.[39] Interleukin 8 (IL-8) is a pro-inflammatory cytokine secreted by both keratinocytes and fibroblasts. IL-8 has a direct effect on immune cells, leading to neutrophil migration, an integral part of the cellular innate immune defence. In addition to this, IL-8 may enhance both keratinocyte and fibroblast migration and has been demonstrated to influence wound healing.[40,41] The ability of both IL-6 and IL-8 to drive both inflammation and promote wound healing makes them very interesting indicators for both the induction and the resolution of infection-induced damage at the oral mucosal barrier.

To gain deeper insight into the synergistic relationship between *C.albicans* and *S.aureus*, and further elucidate the role of this synergy in DS, it is desirable to study the interaction of these in an *in vitro* oral barrier model. A three-dimensional structure incorporating multiple cell types into a matrix material encourages cellular crosstalk and spatial interactions, and allows for cellular migration, stratification and matrix remodeling.[42–48] Depending on the desired application, a different onus is placed on the necessary attributes of a successful oral mucosal model. Selection of incorporated cell types and matrix materials are often dependent on the desired application of the model, each with their own merits and shortfalls.[49] OMMs have been frequently validated for the study of tissue invasion and damage upon infection and have proven to be valuable tools when considering the pathogenesis, virulence and treatment of *C.albicans, S.aureus* and other oral pathogens.[48,50–61] Additionally, OMMs containing keratinocytes and fibroblasts have been demonstrated to produce pro-inflammatory cytokines upon stimulation with live pathogens such as *C.albicans*.[48,62,63]

Few oral mucosal models have gone beyond this, to incorporate immune cells. Those that have been developed included Macrophages and Langerhans cells, however to the best of our knowledge, none have been further implemented for the study of pathogen-host interactions.[62,64–67] Models with the ability to recognise and effectively respond to infection would be informative tools to determine pathogen-host interactions. It is therefore of particular interest to identify any barriers in the current field that may hinder the effective development and implementation of an immunocompetent oral mucosal infection model.

Aims

This paper aims to consider the suitability of a newly devised OMM to model Denture Stomatitis by ensuring that the model effectively represents pathogen-host interactions upon single and dual infections of *C.albicans* and / or *S.aureus*. The immunogenicity of the model environment and its incorporated cell types will be studied, to determine whether the model can produce pro-inflammatory cytokines (IL-6 and IL-8) in response to microbial insult. These data will be used to comment on whether the model environment is a) suitable for the study of pathogen-host interactions at mucosal surface and b) identify the barriers to the further development and application of oral mucosal infection models.

Methodology

Cell selection

HaCaT cells, a spontaneously immortalised keratinocyte cell line, derived from histologically normal adult skin, were employed form the epithelial barrier. HaCaT were selected due to their longevity, reproducibility, reported ability to form stratified, keratinised epithelia and previous employment to represent the inflammatory response of the oral epithelium.[68–71] Human gingival fibroblasts (HGF) were selected to form the lamina propria layer of the tissue when embedded in a type-1 collagen matrix. HGFs were selected due to their anatomical location, as fibroblasts from different locations, even within the oral cavity, are physiologically diverse, and their activity is dependent on their origin.[53,72]

Cell culture

Immortalised keratinocytes (HaCaT), ATCC PCS-200-011 and Primary Human Gingival Fibroblasts (HGF), ATCC PCS-201-018, were maintained in DMEM containing 1 g/L glucose, 584 mg/L L-glutamine, 110 mg/L sodium pyruvate and 15 mg/L phenol red, Life technologies Ltd, Gibco, Paisley UK, and 10% FBS, Life technologies Ltd, Gibco, 10500 batch #08Q1379K. HaCaT were utilised between passages 39 and 48 and HGF, passages 8–14.

OMM production

Three-dimensional oral mucosal models (OMM) were formed in 0.4 µm polycarbonate mesh transwell inserts, Sigma Aldrich, Corning, Gillingham, UK, using rat-tail type-1 collagen, First link (UK) Ltd., Birmingham, UK, with a protein concentration of 2 mg/ml. HGF were embedded into a collagen gel mix, containing: 25.6% collagen, 63.5% DMEM, 7% FBS and 3.8% 1 M NaOH. Once polymerised, a keratinocyte (HaCaT) overlay was added to the gel matrix. Each model was formed of 800 µl total hydrogel mix containing 3.75×10^4 HGF and overlayed with 2.1×10^5 HaCaT. Once the models had contracted (~48 h), remaining media was aspirated and replaced with 500 µl of KGM: Keratinocyte gold basal media, Lonza, Slough, UK, supplemented with KGM gold bullet kit, Lonza (omitting Gentamicin/Amphotericin) and 2.4 µM $CaCl_2$, below the transwell insert. Models were kept at the air-liquid interface (ALI) for the remainder of culture, media was changed every 48–72 h thereafter.

Histology

Formalin fixed paraffin embedded sections (5 µm thickness) were prepared and stained with Haematoxylin and Eosin prior to being mounted using DPX, and imaged.

Microbial preparation

The commonly used strain *C.albicans SC5314* was used alongside a *S.aureus* strain (UOPOSA001), which was isolated from the oral cavity of an individual that wore dentures. Ethical approval and written informed consent were sought to isolate clinically relevant strains of *S.aureus* (Granted by the Health Research Authority London – Camden & Kings Cross Research Ethics Committee, IRAS ref. 208291). A swab was taken from the hard palate and a streak plate performed on mannitol salt agar (MSA), OXOID, Basingstoke, UK. After 24 h of incubation at 37°C a single colony was isolated and transferred onto tryptic-soy agar (TSA) Sigma Aldrich. The pure colony was identified as *S.aureus* through its golden appearance on MSA, positive gram stain and both coagulase positive and catalase positive biochemical tests as per the manufacturer's instructions. Fisher Scientific, Loughborough, UK.

C.albicans was maintained on Sabouraud-dextrose agar, Sigma Aldrich, and *S.aureus* was maintained on TSA. Prior to use, an overnight culture was created by resuspending a single colony of *C.albicans* or *S.aureus* in Sabouraud-dextrose broth or tryptic-soy broth, respectively and grown in a 37°C shaking incubator. Prior to use, *C. albicans* was washed three times via centrifugation at $3000 \times g$ for 5 min in PBS. Cultures were diluted 1 in 10 and counted using a haemocytometer. Prior to use, *S. aureus* was washed three times via centrifugation at $10{,}000 \times g$ in PBS and due to its smaller size, was quantified spectrophotometrically, titrated to an OD of 0.2 at 595 nm (~2×10^7 CFU/ml, as revealed by preliminary experimentation), and subsequently diluted to the desired infectious dose.

LDH assay

A time-course was performed to assess LDH release over the duration of 21 days of OMM culture. A Pierce-LDH cytotoxicity assay kit, Thermo-scientific 88953, was used as per the manufacture's instruction. OMM LDH release was controlled against a maximum LDH release control (MC) by lysing OMMs at each time point, as per the manufacturer's instruction. LDH was firstly represented as a percentage of the MC for each time point, and then represented as a percentage of day-1 LDH release.

Quantification of cytokine secretion

Secretion of IL-6 and IL-8 into cell culture supernatants were quantified by sandwich ELISA, using commercially available paired capture and detection antibodies (BD-Biosciences, Wokingham, UK). Capture antibodies were used at 1 µg/ml (BD Biosciences, 554543) and 2 µg/ml (BD Biosciences, 553716) for IL-6 and IL-8,

respectively, and detection antibodies at 0.5 µg/ml (BD Biosciences 554546 and 554718). Protocols were followed according to manufacturer's instructions and compared to standard curves of recombinant human cytokines (using recognised international cytokine standards available from NIBSC, Potter's Bar, UK) between the range of 7 and 5000 pg/ml. Colorimetric development was determined spectrophotometrically by an OPTIMax tuneable microplate reader at 450 nm and analysed by Softmax Pro version 2.4.1 (Molecular Devices Corp., Sunnyvale, CA, USA).

Monolayer infections

HaCaT cells were seeded at a density of 7.1×10^4 / cm^2, HGF cells were seeded at a density of 1.42×10^4 cells/cm^2, seeding densities were selected due to cell size and to proportionally represent the number of each cell type included in the three-dimensional models (below). Both were grown until confluence at 37°C in 12-well plates. *C.albicans* and *S.aureus* were cultured and quantified as above and then set to a count of 5×10^5 CFU/ml in DMEM + 10% FBS. Control wells contained media only, 1 ml of each organism in DMEM + 10% FBS was added to each single infection well. For dual infections 0.5 ml of each organism was added to the same well ~MOI 0.5 for each.

Three-dimensional infections

OMMs were utilised at day 19, to permit time for sufficient model maturation and infected with *C. albicans* SC5314 ~MOI 0.1 (1×10^5 CFU/ml), *S.aureus* P116 ~MOI 1 (1×10^6 CFU/ml), and both *C. albicans* and *S. aureus* MOI 0.05 and MOI 0.5, respectively. Models were used for both ELISA and Histological evaluation, proportions of microbes were selected to be more representative of the proportion of bacteria to yeast found in *in* vitro infections. Organisms were co-cultured with cells/models for 24 h, and supernatant collected for subsequent ELISA analyses. A 24-h culture was selected to balance the ability to detect the initial response of the OMM to both IL-6 and IL-8 in the model supernatant, and to maximise the amount of time *C.albicans* and *S.aureus* had to commence tissue colonisation, prior to risking the model elevating cytokine levels due to hypoxia, from both prolonged culture time and competition for nutrients from introduced microbes. OMMs were then fixed in 4% PFA for >24 h at 4°C prior to histological analysis.

Model interactions

HaCaT cells were seeded at a density of 5.4×10^5 cells/ml and HGF 1.2×10^5 cells/ml and allowed to adhere overnight. Each cell type was stimulated with collagen and supernatant of the other cell type contained within the model. Cells were embedded in collagen as per the OMM protocol, cultured for 24 h prior to supernatant collection by aspiration after centrifugation at $200 \times g$. Supernatant was collected from cultured cell types, at the same seeding density as detailed above introduced to the other cell type in a pulse-chased manner, to ensure that cytokines contained within the conditioned supernatant did not skew the final ELISA readouts. Supernatant was added to the cell line at a 1:1 ratio with culture medium for 4 h, and then removed. Cells were cultured for a further 18 h in refreshed media. Supernatant was then collected and analysed via ELISA.

Results

OMMs are similar in structure to native oral mucosa

Firstly, to ensure that the model would be suitable for the study of tissue invasion, it was important to ensure that the structure of the OMM suitably represented that of the native oral mucosa. Figure 1 demonstrates cross-sections of OMMs at day-19 compared with native oral mucosa. Both tissues exhibit an organised multi-layered epithelium. Epithelial layers are distinct from the lamina propria layer in both models and native tissue. Native oral mucosa appears highly stratified, the OMM displays a level of stratification that is less organised than that of the native oral mucosa, in image D, whereas image C exhibits even lower stratification. Within the lamina propria layer, fibroblasts are identifiable by their haematoxylin-stained nuclei. There are fewer visible nuclei within the lamina propria layer of the OMM compared with the native tissue. At the apical layer of the epithelium, within both the native oral mucosa and the OMM there are fewer nuclei present, and a flattened appearance indicative of squames. Image C indicates the lamina propria and epithelium have separated.

Cell-death and baseline pro-inflammatory production are interlinked

Preliminary experimentation revealed unexpectedly high levels of the pro-inflammatory cytokines IL-6 and IL-8 during model development. It was necessary to further explore this observation to determine (a) what was the cause of this high inflammatory baseline, (b) whether this was likely to inhibit the use of the OMM to model host response to infection and (c), if not, what is the best timepoint in which to utilise this model.

Figure 2 demonstrates a close relationship between IL-6 and IL-8 pro-inflammatory cytokine production, and LDH release. Spearman's rank correlation analysis indicates a strong positive correlation between LDH release and IL-6 production ($r = 0.936$), LDH release and IL-8 production ($r = 0.945$) and IL-6 and IL-8 production ($r = 0.891$; reporting p values of $p = 0.00008$, 0.00005 and 0.00052,

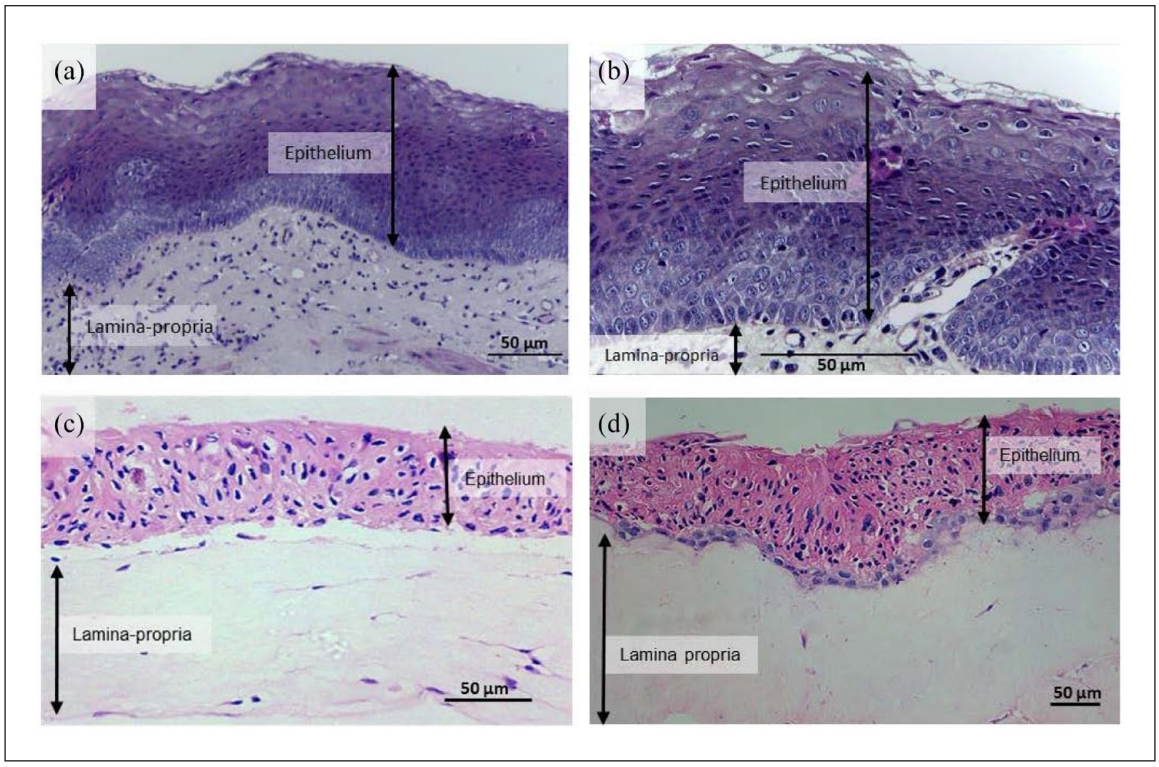

Figure 1. OMMs display histological similarities to native oral mucosal tissue. Images of normal human oral mucosa (a and b) were obtained from: A histopathological image repository of normal epithelium of Oral Cavity and Oral Squamous Cell Carcinoma by Rahman et al.[73], under CC BY 4.0, images were re-oriented, cropped, labelled and post-fitted with a scale bar The two images were selected as they represented a similar field of view to the OMMs formed in this study. A representative sample of paraffin embedded, 4 µm sectioned, haematoxylin and eosin-stained oral mucosal tissue (images c and d) at day 19 of growth (100× magnification) were evaluated. Two images are selected to demonstrate the range of histological presentation of the OMMs and post-fitted with scale bars. Image scale was calculated using pixel size, number of pixels, width of the output image and objective magnification. Labels indicate the epithelial (keratinocyte-containing) and the lamina propria (fibroblast-containing) layers of the tissue.

respectively). A strong correlation is observed between IL-6, IL-8 and LDH release. Higher levels of all factors are observed at day 1, which declines over the first 7 days. After this point the IL-6, IL-8 and LDH activity does not return to its original high level over the 21-day period, however there is gradual increase in all from day 7 onwards. Across all experimental replicates mean IL-6 secretion was 7542.42 ± 1322.65 pg/ml and mean IL-8 secretion was 2481.72 ± 351.4 pg/ml at day 1.

Considering the initial high levels of pro-inflammatory cytokines released upon the formation of the OMMs, it was hypothesised that the introduction of the cell types to the model environment may lead to this marked inflammatory environment. It was therefore of interest to elucidate, if, and if so which components of the model were stimulating which cells to produce such high levels of IL-6 and IL-8.

Collagen and secretory factors affect pro-inflammatory cytokine production

Figure 3 demonstrates that the HaCaT and HGF cell types used to form the OMM react to the matrix environment and soluble factors secreted by the other cell type. Collagen and HGF supernatant upregulated IL-6 production by HaCaT cells, when compared to the unstimulated control ($p = 0.0019$ and < 0.0001, respectively). Conversely, both collagen and HGF supernatant downregulated IL-8 production by HaCaT ($p < 0.0001$ for both). For HGF, IL-6 production was significantly greater when stimulated with collagen, compared with the unstimulated control ($p < 0.0001$), whereas pulse-chasing with HaCaT supernatant demonstrated no significant difference. Both collagen and HaCaT supernatant upregulated IL-8 production by HGF when compared to the unstimulated control ($p < 0.0001$ for both). Across the three experimental replicates, at baseline, the HaCaT unstimulated control produced on average 44.40 ± 26.48 pg/ml of IL-6 and 93.91 ± 41.85 pg/ml of IL-8, and the HGF unstimulated control produced 130.26 ± 72.23 pg/ml of IL-6 and 12.45 ± 6.90 pg/ml of IL-8.

Next, Histological evaluation was used to demonstrate tissue invasion upon infection, and ELISAs demonstrated that models were able to respond to single and dual infections of these microbes. Additionally, following the identification that a variety of unavoidable factors contribute to

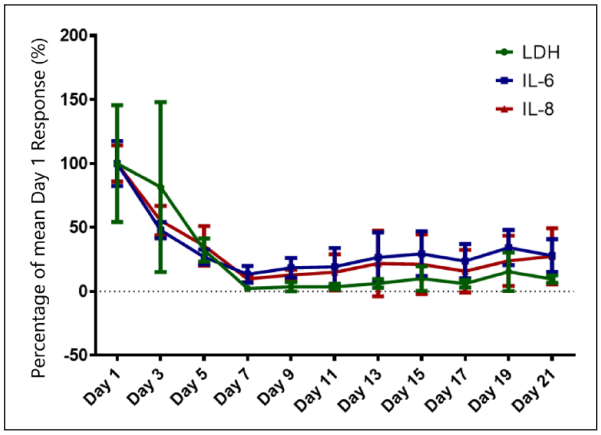

Figure 2. Cell death and IL-6 and IL-8 pro-inflammatory cytokine production correlate across the duration of OMM culture. Three experimental repeats, each with four biological replicates (performed in parallel). LDH activity was controlled using a maximum LDH control at each time point, by lysing models at the same day of growth. IL-6 and IL-8 production were measured via sandwich ELISA. LDH release was normalised to the maximum LDH control for the corresponding time point. LDH, IL-6 and IL-8 values for each time point are reported on this graph as a percentage of mean day 1 release. Data normality was assessed using a Shapiro-Wilk test. Correlation analysis was performed using the non-parametric Spearman's rank correlation test, to determine the relationship between IL-6, IL-8 and LDH release. Error bars represent standard deviation.

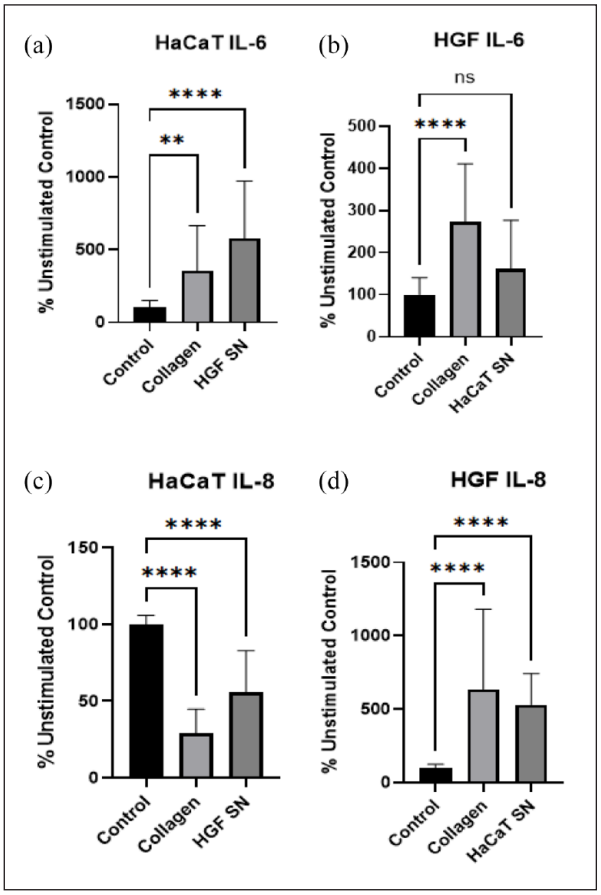

Figure 3. Collagen and conditioned media differentially induce fibroblast and keratinocyte pro-inflammatory cytokines. IL-6 production by HaCaT (a), IL-6 production by HGF (b), IL-8 production by HaCaT (c) and IL-8 production by HGF (d), in response to collagen and supernatant (SN). Supernatant was pulse-chased to ensure that any IL-6 or IL-8 observed by ELISA was because of stimulation by the other incorporated cell-type. Data are from three independent experiments performed in triplicate. Significant differences in cytokine production were compared between the unstimulated control (media only) and stimulated groups. Data normality was assessed using the Shapiro-Wilk test for normality. Statistical significance was determined using a Kruskal-Wallis test followed by a Dunn's multiple comparisons test. Statistical significance is indicated on the graph (*$p < 0.05$. **$p < 0.01$. ***$p < 0.001$. ****$p < 0.0001$, ns = not significant). Error bars represent standard deviation.

the already present IL-6 and IL-8 at the model's baseline, it was next important to determine whether the OMMs were capable of exhibiting upregulation of these cytokines in response to infection with *C.albicans* and *S.aureus*. In addition, it was of interest to determine which, if any, of the two-incorporated cell types were able to recognise and respond to *C.albicans* and *S.aureus*, to gain a more thorough insight of this system and how each cell type may contribute to the overall picture.

OMMs demonstrate tissue-invasion during C.albicans *and* S.aureus *infection*

Within Figure 4, the uninfected control model (a) demonstrates a multi-layered intact epithelium anchored to a lamina-propria that is abundant with fibroblasts. Single *C. albicans* infection (b) can be observed as a layer of hyphae atop the epithelial layer of an intact model. Single infection with *S.aureus* (c) indicates bacteria lining cavities in the lamina-propria of the OMM. Dual infections with both *C. albicans* and *S. aureus* indicate both organisms present on top the epithelium, within the epithelium and within the lamina propria layer (d and e). *C. albicans* formed a layer at the upper most of the section, above the epithelium. *S. aureus* appeared throughout the *Candida* layer. *C. albicans* hyphae span the entire epithelium, with varying biofilm thickness and *S. aureus* can be observed in clusters below this layer. During dual infections, *C.albicans* appears to infrequently penetrate the epithelium (d and e).

C.albicans *and* S.aureus *stimulate pro-inflammatory cytokine production in 2D and 3D culture*

Single and dual infections of *C.albicans* and *S.*aureus stimulated IL-6 and/or IL-8 pro-inflammatory cytokine production by HaCaT and HGF monolayers and OMMs,

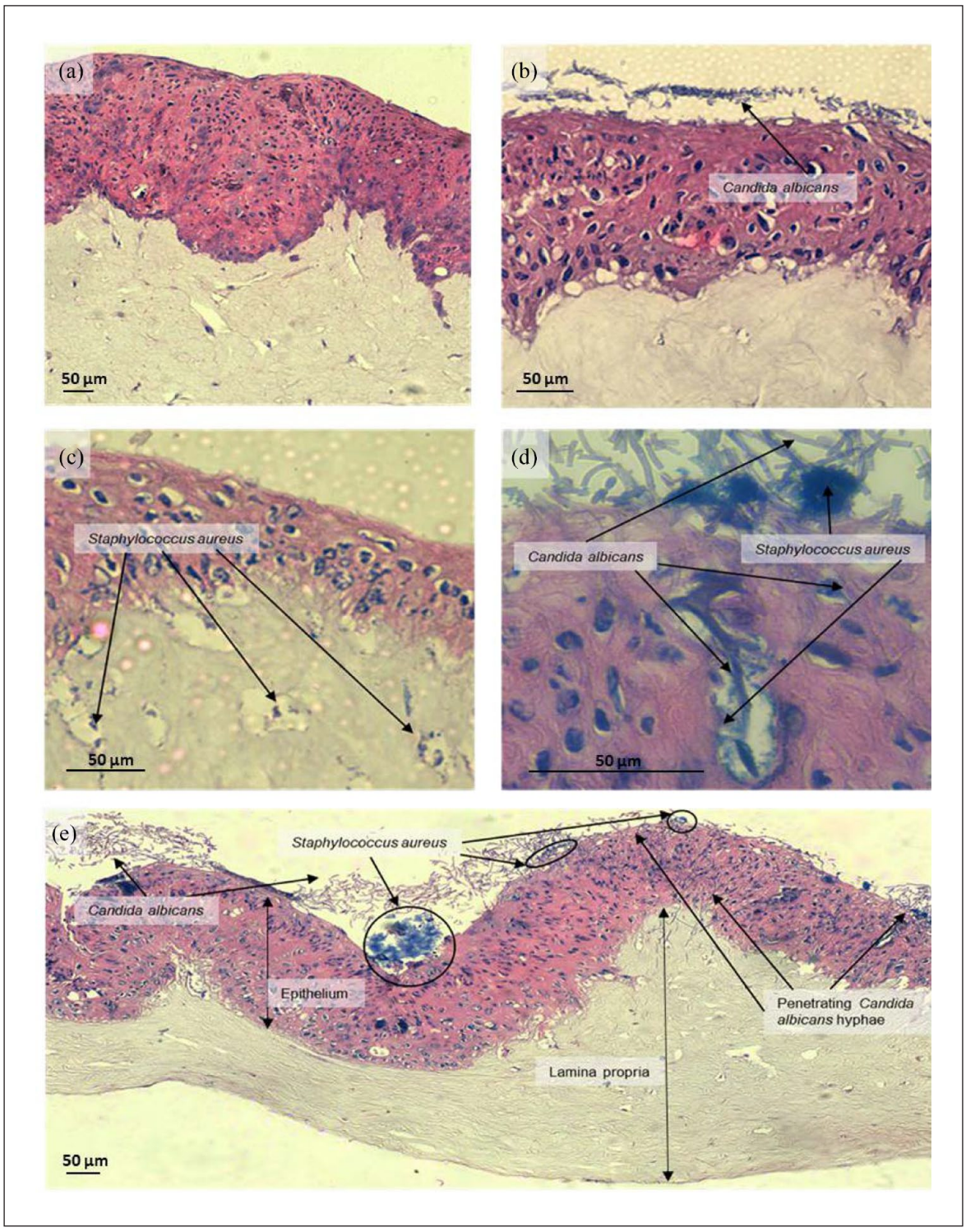

Figure 4. OMMs are suitable to demonstrate biofilm formation and microbial invasion. A representative sample of paraffin embedded, 4 µm sectioned, haematoxylin and eosin stained OMMs infected with *C. albicans* (~MOI 0.1), *S. aureus* (~MOI 1) and both (~MOI 0.05 and 0.5, respectively). Image a displays a control model (100× magnification), in absence of any infection. Image b displays a model infected with *C. albicans* (200× magnification). Image c displays a model infected with *S. aureus* (200× magnification). Image d displays a model infected with both *C. albicans* and *S. aureus* (400× magnification). Image e displays a full-length cross section of an OMM infected with both organisms (100× magnification). Images were post-fitted with scale bars which were calculated using pixel size, number of pixels, width of the output image and objective magnification.

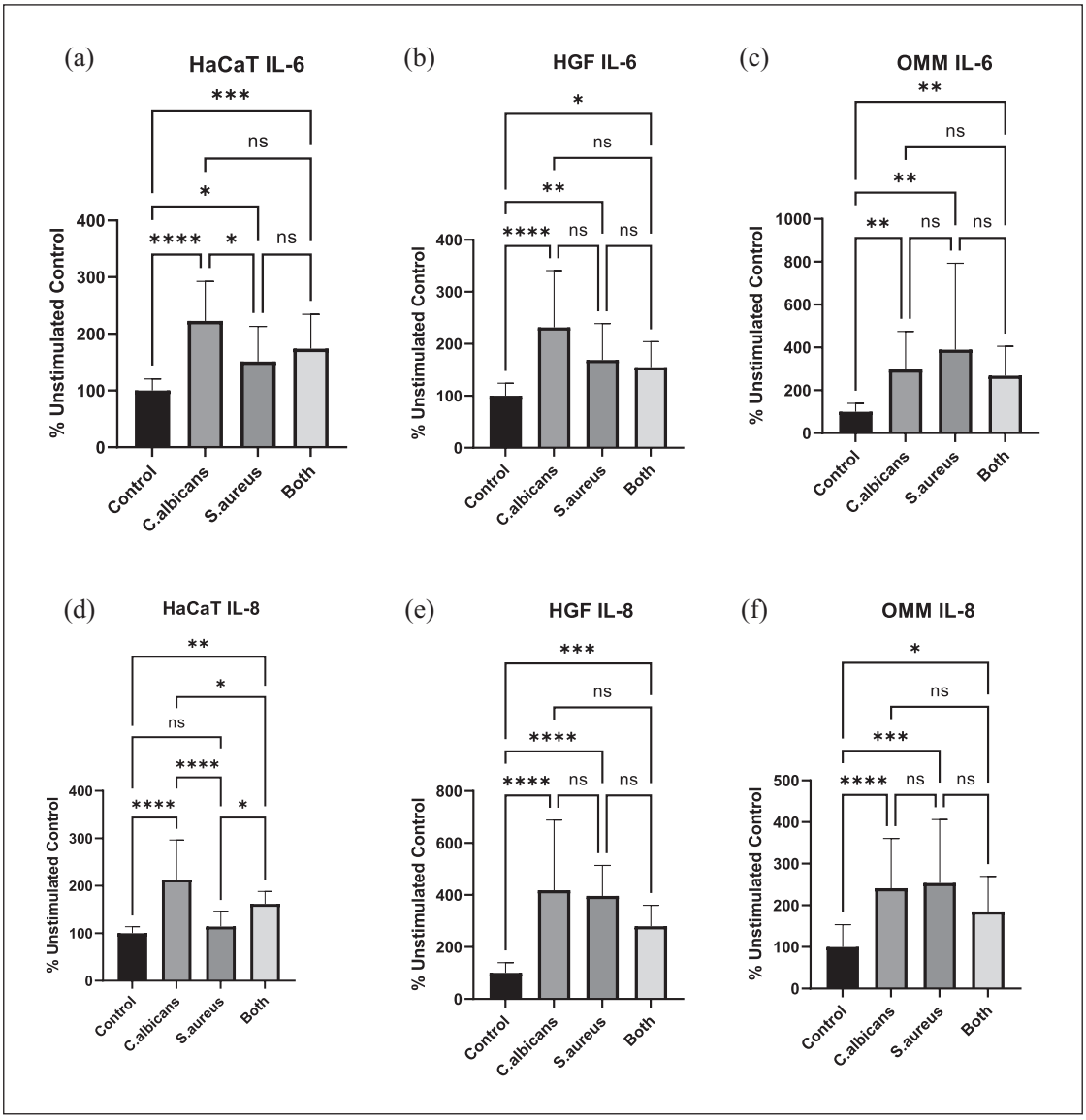

Figure 5. *C.albicans* and *S.aureus* stimulate pro-inflammatory cytokine production by OMMs and individual cell types. IL-6 and IL-8 pro-inflammatory cytokine production by HaCaT (a and d), HGF (b and e) and OMMs (c and f) infected with single infections of *C. albicans* SC5314 and *S. aureus* UOPOSA001, each at a density of 5×10^5 CFU/ml, ~MOI 1 (HaCaT), ~MOI 5 (HGF) and dual infections of both. OMMs were cultured until day 19 and then infected with 1×10^5 CFU/ml *C.albicans* ~MOI 0.1 and 1×10^6 CFU/ml and *S.aureus* ~MOI 1. Dual infections were seeded at half of the amount of each organism. Graphs indicate three experimental repeats performed in triplicate. Models/cells were co-cultured with the infective organisms for 24 h, and cytokine production was assessed via Sandwich ELISA. Data were standardised to the percentage of the unstimulated control group and statistical significance determined between all groups of the same graph. Data normality was assessed using the Shapiro-Wilk test for normality. Statistical significance was determined using a One-Way ANOVA followed by a Dunnett's multiple comparisons test for parametric data (d) or a Kruskal-Wallis followed by a Dunn's multiple comparisons test for (all other) non-parametric data. Statistical significance is indicated on each graph (*$p < 0.05$. **$p < 0.01$. ***$p < 0.001$. ****$p < 0.0001$, NS = Not significant). Error bars represent standard deviation.

when compared to the unstimulated control for each group (Figure 5). *C.albicans* infection significantly increased IL-6 and IL-8 production by HaCaT ($p < 0.0001$ for both). *S.aureus* led to an increase in IL-6, but not IL-8 production within HaCaT cells ($p = 0.0397$ and 0.8171, respectively). Dual infection with both organisms led to a significant increase in both IL-6 and IL-8 production by HaCaT cells ($p = 0.0002$ and 0.0020, respectively). HGF infection with *C.albicans* led to a significant increase in both IL-6 and IL-8 production ($p < 0.0001$ for both). *S.aureus* also significantly increased IL-6 and IL-8 production within HGF ($p = 0.0035$ and < 0.0001, respectively). For HGF, dual

infections of both organisms demonstrated a significant increase in both IL-6 and IL-8 ($p = 0.0175$ and 0.0010, respectively). OMMs infected with *C. albicans*, or *S. aureus*, or dual infections of both microbes led to a significant increase in IL-6 and IL-8 production ($p < 0.0012$, 0.0070 and 0.0015 for IL-6; and $p < 0.0001$, 0.0001 and 0.0312 for IL-8, respectively).

Within HGF cells and OMMs there was no significant difference in either IL-6 or IL-8 production between single and dual infections of *C.albicans* and/or *S.aureus*. However, in HaCaT cells when compared with *S.aureus, C.albicans* was found to stimulate significantly more IL-6 and IL-8 $p = 0.0108$ and < 0.0001, respectively. In addition, for IL-8, dual infections lay somewhere between, stimulating significantly more cytokine production than *S.aureus* alone, $p = 0.0227$, and significantly less than *C.albicans* alone, $p = 0.0121$. This was not observed for IL-6.

Across the three experimental replicates, at baseline, the HaCaT unstimulated control produced an average of 949.82 ± 578.99 pg/ml of IL-6 and 6718.393 ± 4104.485 pg/ml of IL-8, which was highly variable. The HGF unstimulated control produced 1589.99 ± 590.92 pg/ml of IL-6 and 479.202 ± 346.41 pg/ml of IL-8. For OMMs, the baseline was also variable between experimental replicates, on average producing 1511.41 ± 1075.728 pg/ml of IL-6 at baseline and 1258.61 ± 978.279 pg/ml of IL-8.

Discussion

This paper characterises an oral mucosal infection model (OMM) consisting of collagen 1-embedded human gingival fibroblasts (HGF) overlaid with a HaCaT epithelia and explores the potential of this model to accurately represent host-pathogen interactions for the study of oral infections such as denture stomatitis (DS). The OMM characterised formed a simple, effective organotypic full-thickness model that is structurally similar to the native oral mucosa. This model was used to effectively demonstrate tissue-invasion and pro-inflammatory cytokine production in response to the infective agents *Candida albicans* and *Staphylococcus aureus.* Importantly, this work highlighted common challenges and limitations of such models, including their inflammatory baseline, and explores the potential to further develop oral barrier models to further represent the immune system upon infection.

OMMs are robust structures that consistently formed a multi-layered epithelial layer atop a fibroblast populated lamina propria layer, comparable to that of the native oral mucosa. The OMM epithelial layer exhibited less organisation than the highly stratified native oral mucosa. Cells were often denser towards the basal layers of the epithelium, which may indicate a partial stratification. The upper epithelial layers of the 3DOMM indicated a low degree of keratinisation, exhibiting one to two layers of enucleated flattened squames. This lower degree of stratification is due to the use of the immortalised HaCaT cell type.[69] Alternative models utilising primary cells, or h-TERT immortalised cells have achieved stratification that is more comparable to their *in vivo* counterpart.[66,74]

Due to the reduced keratinisation, these models better represent the buccal mucosa as opposed to the hard palate as intended.[75] Considering that the common site for DS infection is that underlying the denture plate, in some cases, such as to model initial DS onset, it may be necessary to consider alternative keratinocyte cell types to better represent the keratinised barrier of a healthy oral mucosa, prior to the introduction of colonised denture-mimics.[59] In future, these models should be stained with laminin, to draw conclusions regarding the ability of HaCaT-HGF OMMs to permit the development of a physiologically relevant basement membrane.[76]

Within an increasing body of literature implementing sophisticated technologies to produce OMMs, this model features towards the more simplistic end of the spectrum. However, with simplicity comes ease of production, affordability and most importantly as demonstrated from our findings, the potential to indicate tissue invasion and cytokine response upon infection. To this model's merit, the epithelial barrier was robust, remaining intact and exhibiting no significant disruption upon pathogenic invasion. This desirable attribute indicates the OMM as a suitable candidate to further elucidate the cellular and molecular mechanisms underpinning DS pathogenesis.

As indicated by the time-course, cell death was at its highest during the first few days of culture, it then declined until day 7, and then steadily rose until day 21. Increased LDH release correlated with high levels of IL-6 and IL-8 and IL-8 pro-inflammatory cytokine production. These elevated levels may be due to uncontrolled cytokine release during cell lysis and damage receptor activation. This particular OMM was used at day-19 to allow enough time for epithelial development and reduce the likelihood of substantial death due to hypoxia if cultured for too long. If models are required for longer-term culture perfusion systems are available to mitigate hypoxia.[77] Considering IL-6 and IL-8 are also known to have roles in cellular migration and matrix remodelling, the observed highly pro-inflammatory baseline may also result from such expected activities during model formation. Considering the above, the length of time a model is left in culture, period of microbial co-culture and timing of supernatant collection from infected models should be carefully balanced.

The incorporated HaCaT and HGF cell types were responsive to both the collagen and secreted factors (supernatant) present in the model environment, mostly inducing a stimulatory effect, increasing IL-6 and/or IL-8 in response to model components, with the exception of collagen and HaCaT cells, which actually led to a reduction in

IL-8 production, even though it still stimulated IL-6 production in this cell type. This already high baseline caused by the model environment did not hinder the model's ability to further respond to pathogens. The differential HaCaT pro-inflammatory response to collagen could be due to the incorporation of cells into the matrix, as opposed to their seeding on top of the matrix when producing the models. This study is not the first to identify that cytokines are differentially expressed between cells cultured in 2D and their collagen-embedded 3D counterparts. In fact, multiple hydrogels including agarose, alginate, collagen, Matrigel and RGD-functionalized polyethylene glycol (PEG) constructs, exhibited differential cytokine expression, this alteration was observed across multiple cell types. Biomaterial properties and cell-type inclusion therefore require thorough consideration when developing a disease model; particularly one where cytokine expression is an intended outcome measure.[78] When selecting model matrices, media and cell-types, it is proposed that attention is paid to the individual responses and crosstalk occurring due to cells being introduced to their new environment.

Standardisation of data to a percentage of the unstimulated baseline without reporting the absolute control values may hinder the appropriate selection of an infection model from the literature. In this study, infected OMMs exhibited varying IL-6 and IL-8 baseline values between the three experimental replicates. Higher baselines demonstrated a less marked upregulation in cytokine production upon infection, compared to replicates with lower baselines. Difficulties may be faced when introducing immune cells to OMMs, due to the ability of cytokines to activate and tailor immune cells such as macrophages towards either a regulatory or inflammatory response.[37] It is also possible that immune-cell crosstalk may help to modulate the model's environment; this remains to be explored. It is therefore proposed that baseline cytokine production should be considered, and that close attention should be paid to cell-matrix interactions if these OMMs, or similar, are taken forward for to further incorporate immune cells.

Pro-inflammatory cytokine production (IL-6 and IL-8) was upregulated in response to both pathogens. These OMMs are therefore likely to be a useful tool for studying a variety of gram-positive bacterial and fungal pathogen-host interactions, due to their ability to produce pro-inflammatory cytokines in response to *C.albicans* and *S.aureus*. However, as the incorporated HaCaT-epithelial cell type are typically unresponsive to LPS and lack expression of the MD-2 adaptor protein, which is required for TLR-4 activation, it should be noted that this model is unlikely to demonstrate a pro-inflammatory cytokine response to gram-negative bacteria.[79] This lack of response is characteristic of barrier cells, due to the necessity of tolerance to maintain homeostasis. In fact, high levels of TLR-4 expression at the skin and mucosal barriers are linked with inflammatory diseases such as systemic sclerosis and periodontitis.[80,81]

It was of particular interest to determine whether this OMM was suitable to model DS with specific reference to the pathogens *C.albicans* and *S.aureus*. This early look demonstrated that *C.*albicans hyphae were able to penetrate the epithelial barrier, and *S.aureus* were subsequently found amongst the lamina propria layer. *C.*albicans can exist as both yeast and hyphal forms. Strain SC5314 is dimorphic but exhibits virulence that can in part be attributed to gene expression that promotes its more invasive, filamentous hyphal form. Yeast to hyphal transition can be promoted by the presence of serum, such as the FBS present in the model environment.[82,83] The OMMs epithelial barrier remained visually intact irrespective of infection with *C.albicans* and / or *S.aureus*. Previous reports have identified significant disruption to the epithelial layer upon *C. albicans* infection of similar full-thickness models with frequent penetration of *Candida* hyphae.[54,56,59] Models were also treated with a higher dose of *C.albicans* SC5315 (MOI 1), and still demonstrated no visible damage to the epithelium (data not shown). Due to this, considering that 24-h incubation with *C. albicans* SC5314 caused obvious epithelial damage in alternative models, it is plausible to consider the epithelia of the newly developed OMM more robust than current alternative infection models.

Models infected with *C. albicans* formed *Candida* biofilms at the surface of the epithelium, regardless of whether *S. aureus* was present. *S.aureus* appeared to line cavities within the lamina propria layer of the OMM regardless of *C.albicans* presence, indicating that *S.aureus* could gain access to deeper tissue layers irrespective of hyphal invasion. However, due to model contraction during culture, *S.aureus* would not have necessarily had to penetrate the epithelial barrier to gain such access and may have entered the construct directly through the lamina propria layer. *C.albicans* hyphal invasion was infrequent and appeared to occur more when *S.aureus* was present. It has been previously reported that the extent and depth of infection with dual species of *C. albicans* and *S. aureus*, were greater than when alone; this was not observed in the present study.[54]

The OMMs and the constituent HaCaT and HGF cell types upregulated pro-inflammatory cytokine production upon infection. However, for HGF and OMMs, no differences in either IL-6 or IL-8 production were observed between single and dual infections of *C. albicans* and *S. aureus*. Within HaCaT cells there was found to be a significant difference in IL-8 production between single and dual infections of *C.albicans* and *S.aureus*, however, this value lay somewhere between that of a single infection with either organism. This could indicate multiple things. It may be the case that these particular strains of synergistic *C.albicans* and *S.aureus* do not exhibit a synergistic response. It may also be the case that regardless of pathogen synergy, host pro-inflammatory cytokine production is not indicative of such. Or, most interestingly, this reduced inflammatory *milieu* could constitute a

synergistic response. If the presence of *C.albicans* reduces inflammation upon *S.aureus* infection, this could prolong the period of time in which *S.aureus* has to evade detection and therefore cross epithelial barriers. Interestingly, the host immune system, namely phagocytosis, appears to play an important role in the synergy between *C.albicans* and *S.aureus* and the subsequent potential for *S.aureus* dissemination.[22] Small colony variants of *S.aureus* have been associated with denture wear. *In vitro, S.aureus* isolates from denture-wearers exhibit enhanced monocyte activation, but reduced phagocytosis when compared to *S.aureus* isolated from non-denture wearers.[13,84] This reduced phagocytosis could promote microbial evasion of the host immune system. Considering that the strain from this study UOPOSA001, is an oral isolate from a denture wearing participant, it is possible that such, or similar suppressive mechanisms may be at play.

The effect of *C. albicans* and *S. aureus* single and dual infections on pro-inflammatory cytokine production has not been frequently reported *in vitro*. In a murine intra-abdominal infection model, and a murine peritonitis model, it was identified that pro-inflammatory cytokine levels (IL-6, GCSF, KC MCP-1 and MIP1α) were elevated in co-infection compared with single infections of *C. albicans* and *S. aureus*.[85] The current findings do not indicate the same, however in a live murine model other cytokine producing cells will be at play, such as macrophages and neutrophils. Within the present study, microbes were only exposed to epithelial and fibroblast cells. It may be the case that upon the further development of the 3DOMM into an immunocompetent model, the pro-inflammatory cytokine balance is shifted upon response to these different combinations of infective agents, due to the ability of multiple cell types to collectively respond. It may also be possible that this synergistic action may be strain dependent. The previously used, well characterised *C.albicans* type strain, SC5314 was used in the present study, alongside a clinical isolate of *S.aureus* (UOPOSA001, IRAS ref. 208291).[54] Due to the relatively recent acceptance of *S.aureus* as an oral coloniser, at the time of experimentation it was difficult to obtain well characterised oral type strains of *S.aureus*. In future, when considering the interactions of these organisms in the context of DS, clinically relevant oral isolates should be used for both strains, to study strains that possess virulence factors that permit oral colonisation. This would allow the study of *C.albicans* and *S.aureus* in a more relevant context and may better represent their proposed synergistic relationship.

Conclusions

Oral mucosal models formed of HaCaT epithelial cells and primary human gingival fibroblasts are suitable for the study of Denture Stomatitis. Models formed reproducible multilayered epithelia, which were suitable for the histological evaluation of cross-kingdom *S.aureus* and *C.albicans* infection. Culturing models for >7 days but <21 days prior to use indicates a suitably low pro-inflammatory baseline to study IL-6 and IL-8 induction upon infection, selecting day 19 to use the models and a 24-h microbial infection maximises the time in which the epithelium can mature. *S.aureus* and *C.albicans* stimulated pro-inflammatory cytokine production by OMMs upon infection but did not exhibit an additive nor deleterious effect when co-cultured. *C.albicans* formed biofilms consisting of hyphae at the epithelial barrier, and infrequently penetrated deeper tissue. *S.aureus* was found in the lamina propria layer of the OMM irrespective of *C.albicans* presence. OMMs produced pro-inflammatory cytokines in response to single and dual infections study of *C.albicans* and *S.aureus*. As such, this OMM proves suitable for the study of gram-positive bacterial and fungal infections at the oral mucosal barrier.

Acknowledgements

The authors wish to thank Mr Matthew Emery, Dr Barbara Durante and Ms *Hélène* Stern for their technical support and advice, Dr Nicole Thomas for the collection of oral swabs, Ms Pam Baxter for advice regarding the IRAS application and Professor Carlos Vergani and Dr Paula Barbugli for their discussions and collaboration in projects prior to this work.

Declaration of conflicting interests

The author(s) declared no potential conflicts of interest with respect to the research, authorship, and/or publication of this article.

Funding

The author(s) disclosed receipt of the following financial support for the research, authorship, and/or publication of this article: This PhD research was funded by a PhD studentship awarded the Peninsula Dental School, University of Plymouth. This research received no specific grant from any funding agency in the public, commercial or not-for-profit sectors.

ORCID iD

Vehid M Salih https://orcid.org/0000-0003-3776-2941

References

1. Cavalcanti YW, Morse DJ, da Silva WJ, et al. Virulence and pathogenicity of Candida albicans is enhanced in biofilms containing oral bacteria. *Biofouling* 2015; 31: 27–38.
2. Naik AV and Pai RC. A study of factors contributing to denture stomatitis in a north Indian community. *Int J Dent* 2011; 2011: 589064.
3. Newton AV. Denture sore mouth a possible etiology. *Br Dent J* 1962; 112: 357–360.
4. Williams DW, Kuriyama T, Silva S, et al. Candida biofilms and oral candidosis: treatment and prevention. *Periodontol* 2011; 55: 250–265.

5. Neppelenbroek KH. The importance of daily removal of the denture biofilm for oral and systemic diseases prevention. *J Appl Oral Sci* 2015; 23: 547–548.
6. Le Bars P, Kouadio AA, Bandiaky ON, et al. Host's immunity and candida species associated with denture stomatitis: a narrative review. *Microorganisms* 2022; 10: 20220716.
7. Pereira-Cenci T, Cury AADB, Crielaard W, et al. Develompent of candida-associated denture stomatitis: new insights. *J Appl Oral Sci* 2008; 16: 86–94.
8. Sumi Y, Kagami H, Ohtsuka Y, et al. High correlation between the bacterial species in denture plaque and pharyngeal microflora. *Gerodontology* 2003; 20: 84–87.
9. Sumi Y, Miura H, Sunakawa M, et al. Colonization of denture plaque by respiratory pathogens in dependent elderly. *Gerodontology* 2002; 19: 25–29.
10. McCormack MG, Smith AJ, Akram AN, et al. Staphylococcus aureus and the oral cavity: an overlooked source of carriage and infection? *Am J Infect Control* 2015; 43: 35–37.
11. Chopde N, Jawale B, Pharande A, et al. Microbial colonization and their relation with potential cofactors in patients with denture stomatitis. *J Contemp Dent Pract* 2012; 13: 456–459.
12. Baena-Monroy T, Moreno-Maldonado V, Franco-Martínez F, et al. Microbial colonization and their relation with potential cofactors in patients with denture stomatitis. *Medicina y Patología Oral* 2005; 10: 27–39.
13. Garbacz K, Kwapisz E and Wierzbowska M. Denture stomatitis associated with small-colony variants of Staphylococcus aureus: a case report. *BMC Oral Health* 2019; 19: 219.
14. Minasyan H. Sepsis: mechanisms of bacterial injury to the patient. *Scand J Trauma Resusc Emerg Med* 2019; 27: 20190214.
15. Carlson E and Johnson G. Protection by Candida albicans of Staphylococcus aureus in the Establishment of Dual Infection in Mice. *Infect Immun* 1985; 50: 655–659.
16. Harriott MM and Noverr MC. Candida albicans and Staphylococcus aureus form polymicrobial biofilms: effects on antimicrobial resistance. *Antimicrob Agents Chemother* 2009; 53: 3914–3922.
17. Schlecht LM, Peters BM, Krom BP, et al. Systemic Staphylococcus aureus infection mediated by Candida albicans hyphal invasion of mucosal tissue. *Microbiology* 2015; 161: 168–181.
18. del Rio A, Cervera C, Moreno A, et al. Patients at risk of complications of Staphylococcus aureus bloodstream infection. *Clin Infect Dis* 2009; 48(Suppl 4): S246–253.
19. Peters BM, Ovchinnikova ES, Krom BP, et al. Staphylococcus aureus adherence to Candida albicans hyphae is mediated by the hyphal adhesin Als3p. *Microbiology* 2012; 158: 2975–2986.
20. Scheller J, Chalaris A, Schmidt-Arras D, et al. The pro- and anti-inflammatory properties of the cytokine interleukin-6. *Biochim Biophys Acta* 2011; 1813: 878–888.
21. Smith AJ, Brewer A, Kirkpatrick P, et al. Staphylococcal species in the oral cavity from patients in a regional burns unit. *J Hosp Infect* 2003; 55: 184–189.
22. Van Dyck K, Viela F, Mathelie-Guinlet M, et al. Adhesion of staphylococcus aureus to candida albicans during co-infection promotes bacterial dissemination through the host immune response. *Front Cell Infect Microbiol* 2020; 10: 624839.
23. Biondo C, Malara A, Costa A, et al. Recognition of fungal RNA by TLR7 has a nonredundant role in host defense against experimental candidiasis. *Eur J Immunol* 2012; 42: 2632–2643.
24. Bishop CT, Blank F and Gardner PE. The cell wall polysaccharides of candida albicans, glucan, mannan, and chitin. *Can J Chem* 1960; 38: 869–881.
25. Cohen-Kedar S, Baram L, Elad H, et al. Human intestinal epithelial cells respond to beta-glucans via Dectin-1 and Syk. *Eur J Immunol* 2014; 44: 3729–3740.
26. Gow NA, van de Veerdonk FL, Brown AJ, et al. Candida albicans morphogenesis and host defence: discriminating invasion from colonization. *Nat Rev Microbiol* 2011; 10: 112–122.
27. Miyazato A, Nakamura K, Yamamoto N, et al. Toll-like receptor 9-dependent activation of myeloid dendritic cells by Deoxynucleic acids from Candida albicans. *Infect Immun* 2009; 77: 3056–3064.
28. Netea MG, van de Veerdonk F, Verschueren I, et al. Role of TLR1 and TLR6 in the host defense against disseminated candidiasis. *FEMS Immunol Med Microbiol* 2008; 52: 118–123.
29. Tada H, Nemoto E, Shimauchi H, et al. Saccharomyces cerevisiae- and Candida albicans-derived mannan induced production of tumor necrosis factor alpha by human monocytes in a CD14- and Toll-like receptor 4-dependent manner. *Microbiol Immunol* 2002; 46: 503–512.
30. Wagener J, Mailänder-Sanchez D and Schaller M (2012) Immune Responses to Candida albicans in Models of In Vitro Reconstituted Human Oral Epithelium. In: Brand, A., MacCallum, D. (eds) *Host-Fungus Interactions. Methods in Molecular Biology* (vol 845., pp333–344) Totowa, NJ: Humana.
31. Zheng NX, Wang Y, Hu DD, et al. The role of pattern recognition receptors in the innate recognition of Candida albicans. *Virulence* 2015; 6: 347–361.
32. Fournier B and Philpott DJ. Recognition of Staphylococcus aureus by the innate immune system. *Clin Microbiol Rev* 2005; 18: 521–540.
33. Takeda K, Takeuchi O and Akira S. Recognition of lipopeptides by Toll-like receptors. *J Endotoxin Res* 2002; 8: 459–463.
34. Jouault T, Ibata-Ombetta S, Takeuchi O, et al. Candida albicans phospholipomannan is sensed through Toll-like receptors. *J Infect Dis* 2003; 188: 165–172.
35. Ozinsky A, Underhill DM, Fontenot JD, et al. The repertoire for pattern recognition of pathogens by the innate immune system is defined by cooperation between Toll-like receptors. *PNAS* 2000; 97: 13766–13771.
36. Fukui A, Ohta K, Nishi H, et al. Interleukin-8 and CXCL10 expression in oral keratinocytes and fibroblasts via Toll-like receptors. *Microbiol Immunol* 2013; 57: 198–206.
37. Metcalfe S, Anselmi N, Escobar A, et al. Innate phagocyte polarization in the oral cavity. *Front Immunol* 2021; 12: 768479.
38. Tanaka T, Narazaki M and Kishimoto T. IL-6 in inflammation, immunity, and disease. *Cold Spring Harb Perspect Biol* 2014; 6: a016295.
39. Johnson BZ, Stevenson AW, Prele CM, et al. The role of IL-6 in skin fibrosis and cutaneous wound healing. *Biomedicines* 2020; 8: 20200430.
40. Rennekampff HO, Hansbrough JF, Kiessig V, et al. Bioactive interleukin-8 is expressed in wounds and enhances wound healing. *J Surg Res* 2000; 93: 41–54.

41. Jiang WG, Sanders AJ, Ruge F, et al. Influence of interleukin-8 (IL-8) and IL-8 receptors on the migration of human keratinocytes, the role of PLC-gamma and potential clinical implications. *Exp Ther Med* 2012; 3: 231–236.
42. Conti HR, Huppler AR, Whibley N, et al. Animal models for candidiasis. *Curr Protoc Immunol* 2014; 105: 19.6.1-19.6.17.
43. Caddeo S, Boffito M and Sartori S. Tissue engineering approaches in the design of healthy and pathological in vitro tissue models. *Front Bioeng Biotechnol* 2017; 5: 40.
44. Colley HE, Hearnden V, Jones AV, et al. Development of tissue-engineered models of oral dysplasia and early invasive oral squamous cell carcinoma. *Br J Cancer* 2011; 105: 1582–1592.
45. Ghahary A and Ghaffari A. Role of keratinocyte-fibroblast cross-talk in development of hypertrophic scar. *Wound Repair Regen* 2007; 15(Suppl 1): S46–S53.
46. Torras N, Garcia-Diaz M, Fernandez-Majada V, et al. Mimicking epithelial tissues in three-dimensional cell culture models. *Front Bioeng Biotechnol* 2018; 6: 197.
47. Wojtowicz AM, Oliveira S, Carlson MW, et al. The importance of both fibroblasts and keratinocytes in a bilayered living cellular construct used in wound healing. *Wound Repair Regen* 2014; 22: 246–255.
48. Yadev NP, Murdoch C, Saville SP, et al. Evaluation of tissue engineered models of the oral mucosa to investigate oral candidiasis. *Microb Pathog* 2011; 50: 278–285.
49. Abou Neel EA, Chrzanowski W, Salih VM, et al. Tissue engineering in dentistry. *J Dent* 2014; 42: 915–928.
50. Bouabe H, Okkenhaug K. Virus-host interactions. In: Walker JM (ed.) *Methods in molecular biology* (pp.1064: 315-336). New York: Springer, 2013.
51. Bugueno IM, Batool F, Keller L, et al. Porphyromonas gingivalis bypasses epithelial barrier and modulates fibroblastic inflammatory response in an in vitro 3D spheroid model. *Sci Rep* 2018; 8: 1–13.
52. Chaudhari AA, Joshi S, Vig K, et al. A three-dimensional human skin model to evaluate the inhibition of Staphylococcus aureus by antimicrobial peptide-functionalized silver carbon nanotubes. *J Biomater Appl* 2019; 33: 924–934.
53. Dabija-Wolter G, Bakken V, Cimpan MR, et al. In vitro reconstruction of human junctional and sulcular epithelium. *J Oral Pathol Med* 2013; 42: 396–404.
54. de Carvalho Dias K, de Sousa DL, Barbugli PA, et al. Development and characterization of a 3D oral mucosa model as a tool for host-pathogen interactions. *J Microbiol Methods* 2018; 152: 52–60.
55. De Ryck T, Grootaert C, Jaspaert L, et al. Development of an oral mucosa model to study host-microbiome interactions during wound healing. *Appl Microbiol Biotechnol* 2014; 98: 6831–6846.
56. Dongari-Bagtzoglou A and Kashleva H. Development of a highly reproducible three-dimensional organotypic model of the oral mucosa. *Nat Protoc* 2006; 1: 2012–2018.
57. Hogk I, Kaufmann M, Finkelmeier D, et al. An in vitro HSV-1 reactivation model containing quiescently infected PC12 cells. *Biores Open Access* 2013; 2: 250–257.
58. Shepherd J, Douglas I, Rimmer S, et al. Development of three-dimensional tissue-engineered models of bacterial infected human skin wounds. *Tissue Eng Part C Methods* 2009; 15: 475–484.
59. Morse DJ, Wilson MJ, Wei X, et al. Denture-associated biofilm infection in three-dimensional oral mucosal tissue models. *J Med Microbiol* 2018; 67: 364–375.
60. Reddersen K, Wiegand C, Elsner P, et al. Three-dimensional human skin model infected with Staphylococcus aureus as a tool for evaluation of bioactivity and biocompatibility of antiseptics. *Int J Antimicrob Agents* 2019; 54: 283–291.
61. Ren X, van der Mei HC, Ren Y, et al. Keratinocytes protect soft-tissue integration of dental implant materials against bacterial challenges in a 3D-tissue infection model. *Acta Biomater* 2019; 96: 237–246.
62. Pimentel B, Marin-Dett FH, Assis M, et al. Antifungal activity and biocompatibility of alpha-AgVO(3), alpha-Ag(2)WO(4), and beta-Ag(2)MoO(4) using a three-dimensional coculture model of the oral mucosa. *Front Bioeng Biotechnol* 2022; 10: 826123.
63. Whiley RA, Cruchley AT, Gore C, et al. Candida albicans strain-dependent modulation of pro-inflammatory cytokine release by in vitro oral and vaginal mucosal models. *Cytokine* 2012; 57: 89–97.
64. Bechetoille N, Vachon H, Gaydon A, et al. A new organotypic model containing dermal-type macrophages. *Exp Dermatol* 2011; 20: 1035–1037.
65. Linde N, Gutschalk CM, Hoffmann C, et al. Integrating macrophages into organotypic co-cultures: a 3D in vitro model to study tumor-associated macrophages. *PLoS ONE* 2012; 7: e40058.
66. Ollington B, Colley HE and Murdoch C. Immunoresponsive tissue-engineered oral mucosal equivalents containing macrophages. *Tissue Eng Part C Methods* 2021; 27: 462–471.
67. Sivard P, Dezutter-Dambuyant C, Kanitakis J, et al. In vitro reconstructed mucosa-integrating Langerhans' cells. *Exp Dermatol* 2003; 12: 346–355.
68. Jung MH, Jung SM and Shin HS. Co-stimulation of HaCaT keratinization with mechanical stress and air-exposure using a novel 3D culture device. *Sci Rep* 2016; 6: 33889.
69. Maas-Szabowski N, Starker A and Fusenig NE. Epidermal tissue regeneration and stromal interaction in HaCaT cells is initiated by TGF-alpha. *J Cell Sci* 2003; 116: 2937–2948.
70. Colombo I, Sangiovanni E, Maggio R, et al. HaCaT cells as a reliable in vitro differentiation model to dissect the inflammatory/repair response of human keratinocytes. *Mediators Inflamm* 2017; 2017: 7435621.
71. Gursoy UK, Gursoy M, Kononen E, et al. Construction and characterization of a multilayered gingival keratinocyte culture model: the TURK-U model. *Cytotechnology* 2016; 68: 2345–2354.
72. Nolte SV, Xu W, Rennekampff HO, et al. Diversity of fibroblasts—a review on implications for skin tissue engineering. *Cells Tissues Organs* 2008; 187: 165–176.
73. Rahman TY, Mahanta LB, Das AK, et al. Histopathological imaging database for oral cancer analysis. *Data Brief* 2020; 29: 105114.
74. Jennings Luke R., Colley Helen E., Ong Jane, et al. Development and characterization of in vitro human oral mucosal equivalents derived from immortalized oral keratinocytes. *Tissue Eng Part C Methods* 2016; 2016: 1108–1117.
75. Groeger S and Meyle J. Oral mucosal epithelial cells. *Front Immunol* 2019; 10: 208.
76. Timpl R. Structure and biological activity of basement membrane proteins. *Eur J Biochem* 1989; 180: 487–502.

77. Schmid J, Schwarz S, Meier-Staude R, et al. A perfusion bioreactor system for cell seeding and oxygen-controlled cultivation of three-dimensional cell cultures. *Tissue Eng Part C Methods* 2018; 24: 585–595.
78. Regier MC, Montanez-Sauri SI, Schwartz MP, et al. The influence of biomaterials on cytokine production in 3D cultures. *Biomacromolecules* 2017; 18: 709–718.
79. Kollisch G, Kalali BN, Voelcker V, et al. Various members of the Toll-like receptor family contribute to the innate immune response of human epidermal keratinocytes. *Immunology* 2005; 114: 531–541.
80. Qi W, Yang X, Ye N, et al. TLR4 gene in the regulation of periodontitis and its molecular mechanism. *Exp Ther Med* 2019; 18: 1961–1966.
81. Stifano G, Affandi AJ, Mathes AL, et al. Chronic Toll-like receptor 4 stimulation in skin induces inflammation, macrophage activation, transforming growth factor beta signature gene expression, and fibrosis. *Arthiritis Res Ther* 2014; 16: 1–13.
82. Hua H, Yuan X, Mitchell BM, et al. Morphogenic and genetic differences between Candida albicans strains are associated with keratomycosis virulence. *Mol Vis* 2009; 15: 1476–1484.
83. Samaranayake YH, Cheung BP, Yau JY, et al. Human serum promotes Candida albicans biofilm growth and virulence gene expression on silicone biomaterial. *PLoS One* 2013; 8: e62902.
84. Garbacz K, Jarzembowski T, Kwapisz E, et al. Do the oral Staphylococcus aureus strains from denture wearers have a greater pathogenicity potential? *J Oral Microbiol* 2019; 11: 1536193.
85. Peters BM and Noverr MC. Candida albicans-Staphylococcus aureus polymicrobial peritonitis modulates host innate immunity. *Infect Immun* 2013; 81: 2178–2189.